



**Western Region Technical Attachment
No. 95-11
April 11, 1995**

**DOPPLER RADAR IDENTIFICATION OF A
SUPERCCELL THUNDERSTORM IN THE IDAHO MOUNTAINS**

**Michael C. Conger, David R. Sanders and Lawrence B. Dunn
NWSFO Salt Lake City, Utah**

Introduction

The character of severe local storms (tornadoes, large hail, and winds ≥ 50 knots) over the western United States differ significantly from severe storms over the East. Over the West, "dry" microbursts associated with the Beebe Type IV (inverted-V) sounding (Beebe 1955) are the most common severe storms. Tornadoes and large hail do occur over the western mountains, though the frequency of occurrence is uncertain due to the low population density. Typically, western storms are less intense and of shorter duration than their eastern counterparts. A notable exception was an F4 tornado in Yellowstone National Park in 1987 (Fujita 1989).

A key element in the development of deep, sustained convection favorable for severe thunderstorm formation is environmental wind shear. In areas east of the Continental Divide, certain vertical wind profiles are commonly associated with severe local convection. These same wind profiles are harder to identify in the West due to complications resulting from complex terrain in the boundary layer and little or no surface data in the mountainous areas. Conventional upper-air observations from rawinsondes and Doppler wind profilers do well in identifying vertical shear above the boundary layer. However, these same observing methods are inadequate for locating inflow into thunderstorms occurring within mountainous terrain.

Doppler velocity/reflectivity data from the WSR-88D provide a means to identify mesoscale features associated with severe local storms. The potential for storms to produce severe weather can now be evaluated using the radar data, even over mountainous terrain where surface data is often not available. In this Technical Attachment, Doppler velocity and reflectivity data will show a classic supercell thunderstorm structure not seen before in radar data over the western mountains. Base radar data from the Boise WSR-88D will be evaluated using the non-associated PUP at the CBRFC in Salt Lake City. PCGRIDS and SHARP software will also be used to produce 0000 UTC model and rawinsonde output, respectively.

Synopsis

At 0000 UTC, 8 May 1994, a closed 500 mb low was centered over central California with a southwest-northeast oriented ridge axis across the eastern Pacific Ocean extending into the Pacific Northwest. This resulted in easterly flow across southern Idaho with the flow backing to the northeast across northern Idaho (Fig. 1). In the 6-hour period prior to 0000 UTC, one tornado and a number of severe thunderstorms were reported in the Snake River Valley of

southern Idaho. Quasi-geostrophic (QG) forcing of upward vertical motion at 0000 UTC as determined from the divergence of Q-vectors at 300 mb (Fig. 2) was weak across southern/central Idaho. However, strong divergence of the total wind at 300 mb (Fig. 3a) with an underlying 700 mb convergence area (Fig. 3b) was present. This synoptic scale convergence/ divergence couplet created a favorable convective environment throughout southern/central Idaho.

Shortly after 0000 UTC, an intensifying thunderstorm was detected approximately 60 miles north of the Boise radar in the central mountains near Cascade, Idaho. Movement of the storm was in a general westerly direction. Reflectivity data showed a maximum core value of 50 dBZ at a 1.5° elevation scan (Fig. 4) with a mesocyclone signature evident in the velocity data at the same elevation scan (Fig. 5). This thunderstorm was severe and produced downburst winds strong enough to snap 40-inch diameter trees sometime between 0020 and 0100 UTC.

Case Study

A strong vertically sheared environment favors mature, long-duration storms. Tilted updrafts and coexisting updraft/downdraft couplets found in these storms contribute to the growth of hail and tornado development. A hodograph based on the observed winds from the 0000 UTC Boise, Idaho rawinsonde (Fig. 6) showed the existence of strong vertical shear over western Idaho from the surface to 7000m shortly before the development of the severe thunderstorm. The shear profile suggests any storms that form may be supercells (Weisman and Klemp 1984), but lack of information about the boundary layer winds in the complex terrain adds uncertainty to this statement.

The storm, in this case, showed many of the classic radar characteristics of a supercell thunderstorm. Specifically, the circulation within the storm was large (relative to storm scale), intense, and in a quasi-steady state (≥ 20 minutes) (Browning 1964, 1968). This circulation covered a substantial depth of the atmosphere. Elevation scans at 0.5° (≈ 3000 m MSL) and 1.5° (≈ 4000 m MSL) showed a well-defined mesocyclone which persists through the 2.4° (≈ 5500 m MSL) elevation scan, and weakly up to 3.4° (≈ 8000 m MSL) (Figs. 7a-d). The mesocyclone was relatively intense with a radial velocity maximum $(\mathbf{v}_R) = (\mathbf{v}_T - \mathbf{v}_O) / 2$ approaching 30 knots around 0041 UTC. A quasi-steady state exists with this storm. Time lapsed velocity data beginning around 0000 UTC (not shown) showed a persistent mesocyclone over the same general location. In a study of storms with mesocyclones, Burgess (1976) found that 95 percent of the storms produced surface damage, while 62 percent were associated with tornadoes over the Plains states.

Reflectivity data also exhibited supercell structure. The lowest elevation scans (0.5° - 1.5°) had rather weak echo returns (≤ 20 dBZ) near the center of the circulation (Figs. 8a-b). At higher elevation scans (2.4° - 3.4°), the echo return strength increased dramatically with a 50 dBZ return at 3.4° (Figs. 8c-d). This reflectivity profile represents a **weak-echo vault** (or vault) within the supercell (Browning and Ludlam 1962, Browning and Donaldson 1963). A cross section through a typical supercell (Fig. 9) shows the vault region in relation to the low-level inflow. The reason this region has weak radar echoes is that the updrafts are so strong that precipitation does not have time to form until the air parcels have reached high levels in the cloud. This explains the reason the radar echoes are more intense at high elevation

scans near the vault than in the lower elevations. A detailed treatise of weak-echo vaults in supercell thunderstorms is beyond the scope of this paper, though it can be stated that weak-echo vaults are indicative of intense updraft regions which are commonly associated with severe thunderstorms.

Summary

Historically, a number of severe thunderstorms, including those with large hail or tornadoes, have been confirmed in the western mountains. The severe thunderstorm in this case study was not unusual in either its structure or its occurrence over high terrain (though the westward movement of the cell was unusual). Instead, this supercell was identified within mountainous terrain using Doppler reflectivity/velocity data. Prior to the installation of the WSR-88D, a storm such as this would be difficult or impossible to assess in complex terrain.

The WSR-88D now offers the forecaster a means to identify supercell severe storms in real time in data sparse regions of the West. Equally important, the forecaster can now distinguish between the storms with large hail/tornado potential, and the more common airmass or "dry" microburst-type thunderstorm. The ability to separate the two will lead to a better severe weather warning program in the Western Region.

References

- Beebe, R. G., 1955: Types of airmasses in which tornadoes occur. *Bull Amer. Meteor. Soc.*, **36**, 340-50.
- Browning, K. A., 1964: Airflow and precipitation trajectories within severe local storms which travel to the right of the winds. *J. Atmos. Sci.*, **21**, 634-39.
- , 1968: The organization of severe local storms. *Weather*, **23**, 429-34.
- , and R. J. Donaldson, Jr., 1963: Airflow and structure of a tornadic storm. *J. Atmos. Sci.*, **20**, 533-45.
- , and G. B. Foote, 1976: Airflow and hail growth in supercell storms and some implications for hail suppression. *Quart. J. Roy. Meteor. Soc.*, **102**, 499-533.
- , and F. H. Ludlam, 1962: Airflow in convective storms. *Quart. J. Roy. Meteor. Soc.*, **88**, 117-35.
- Burgess, D. W., 1976: Single-Doppler radar vortex recognition: part 1 - mesocyclone signatures. 17th Conf. on Radar Meteorology (Seattle) AMS. Preprint, pp. 97-103. Boston, American Meteorological Society.
- Fujita, T. T., 1989: The Teton-Yellowstone Tornado of 21 July 1987. *Mon. Wea. Rev.*, **117**, 1913-40.
- Weisman, M. L., and J. B. Klemp, 1984: The structure and classification of numerically simulated convective storms in directionally varying shears. *Mon. Wea. Rev.*, **112**, 2479-98.

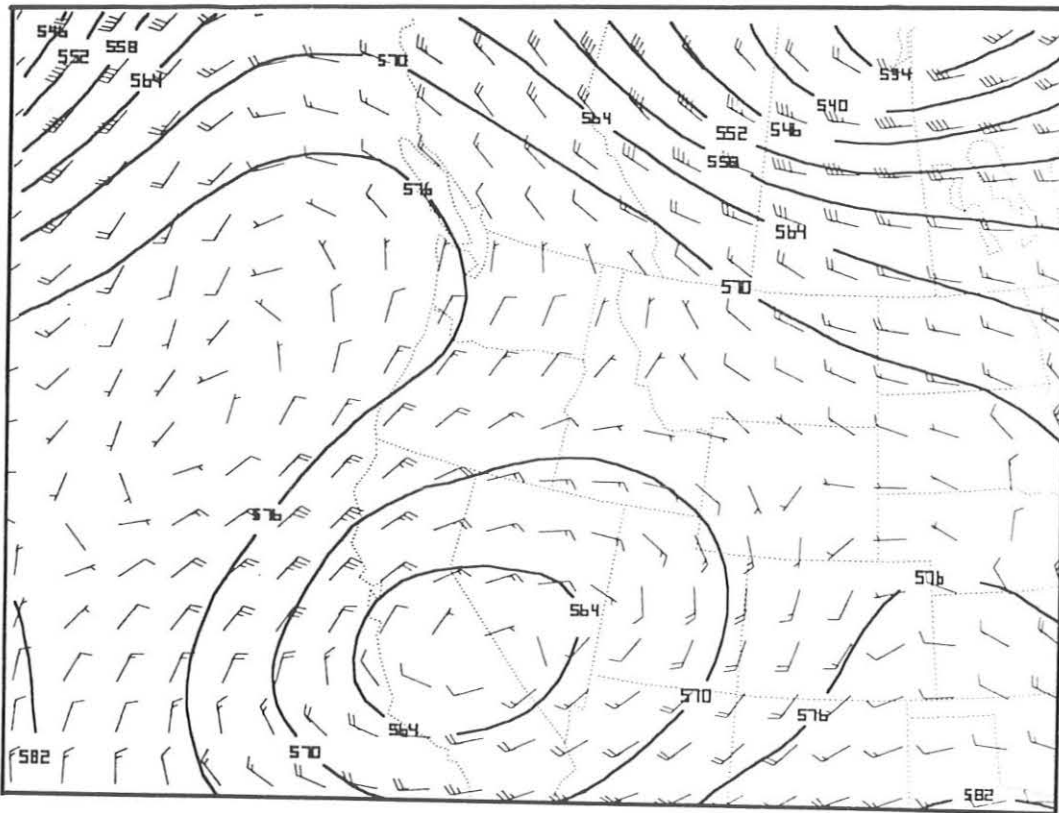


Figure 1. NGM 0000 UTC, 8 May, 1994 00 hour forecast of 500 mb heights (6 dam) and winds (m s^{-1}).

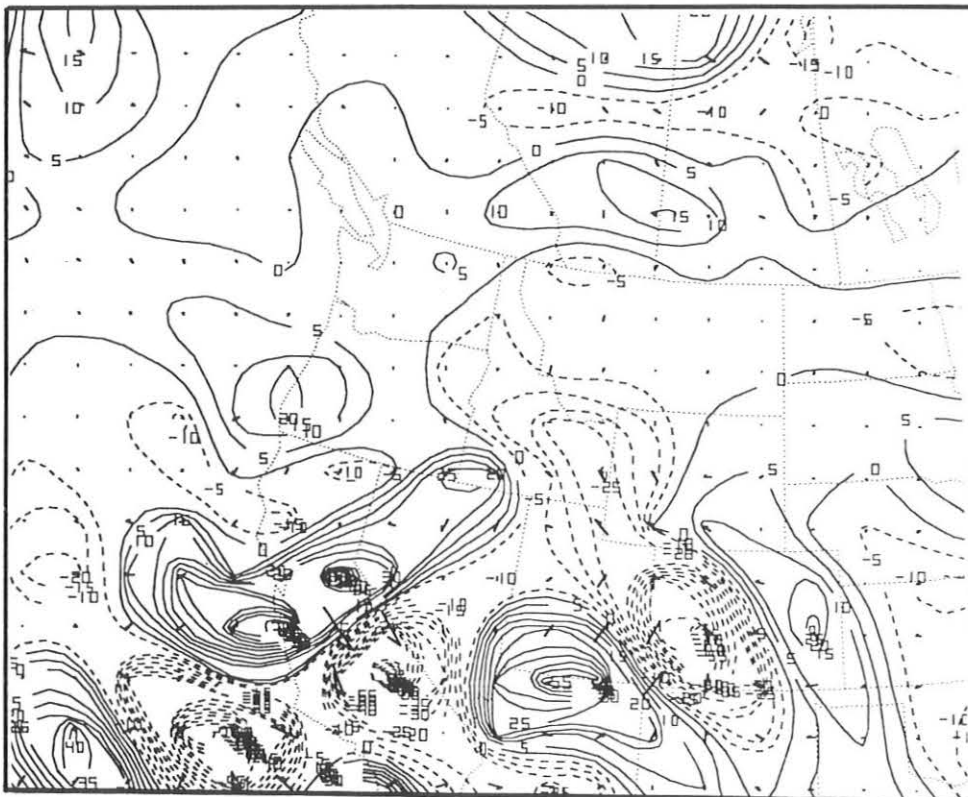


Figure 2. NGM 0000 UTC, 8 May, 1994 00 hour forecast of divergence of Q-vectors ($\nabla \cdot \mathbf{Q}$) at 300 mb. Dashed (solid) contours represent convergence (divergence) of Q which corresponds to upward (downward) motion. Contour intervals $5 \times 10^{10} \text{mb}^{-1} \text{s}^{-3}$. Small arrows represent Q-vectors.

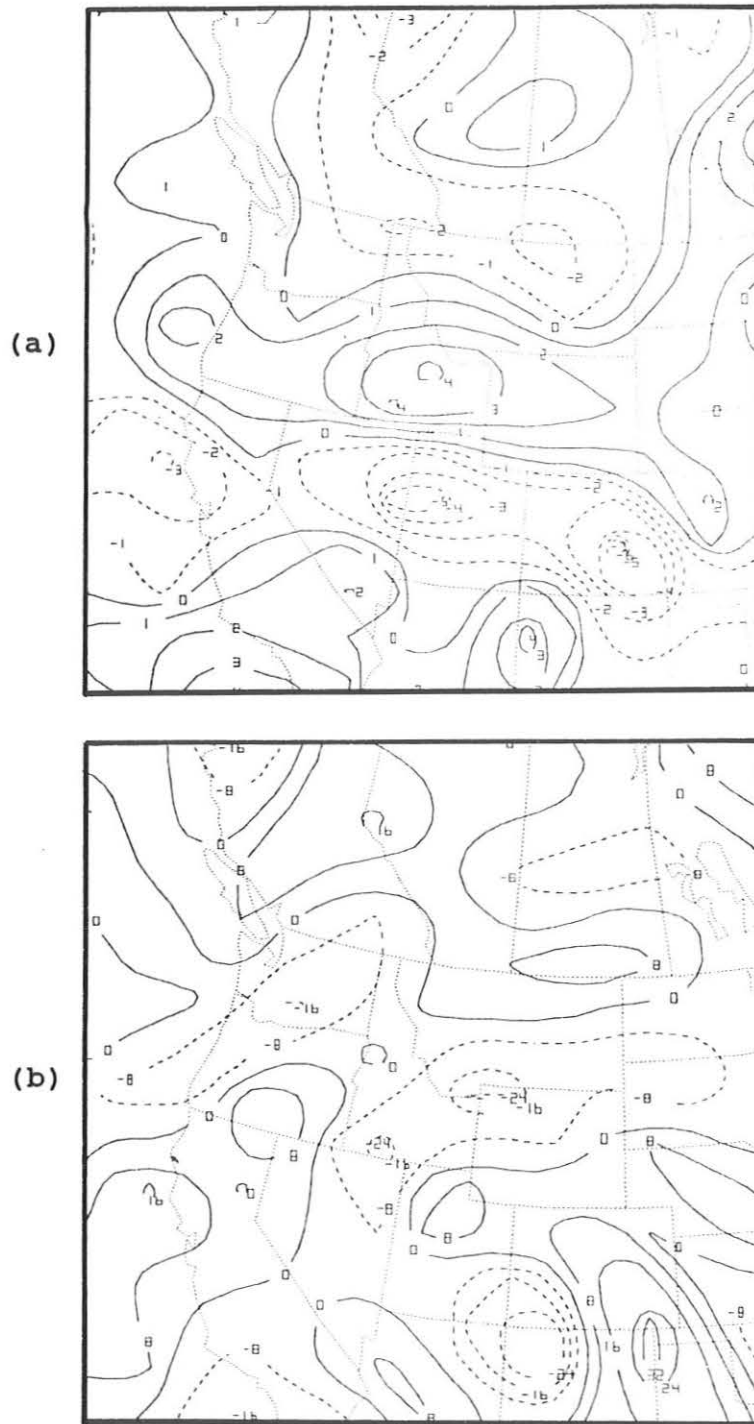


Figure 3. NGM 0000 UTC, 8 May, 1994 00 hour forecast of total wind divergence at (a) 300 mb, and (b) 700 mb. Positive (negative) values indicate divergence (convergence). Contour intervals $1 \times 10^{-5} \text{ s}^{-1}$ in (a) and $8 \times 10^{-6} \text{ s}^{-1}$ in (b).

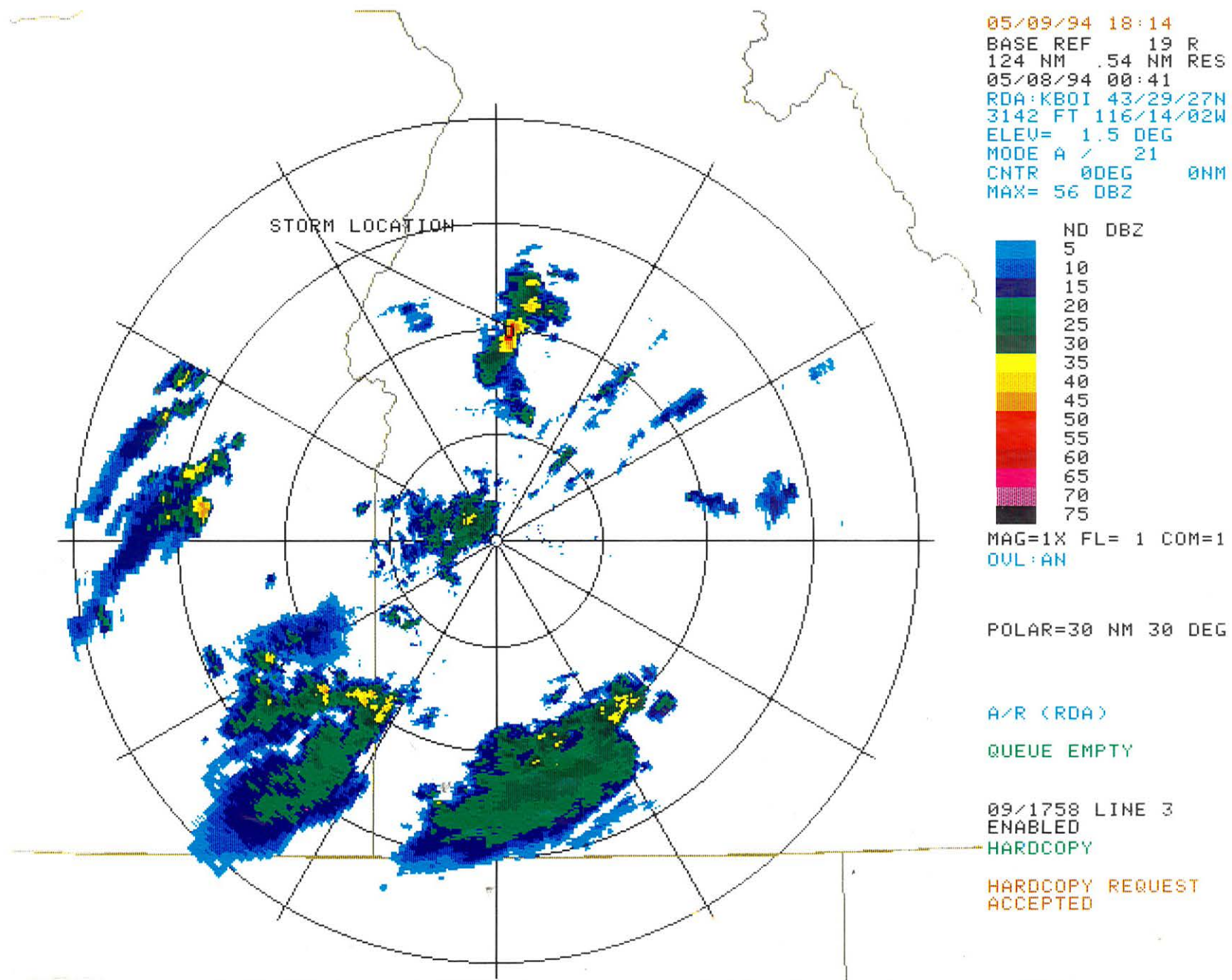


Figure 4. Base reflectivity data from the Boise WSR-88D at 0041 UTC, 8 May 1994. Elevation scan 1.5°. Range rings 30 km.

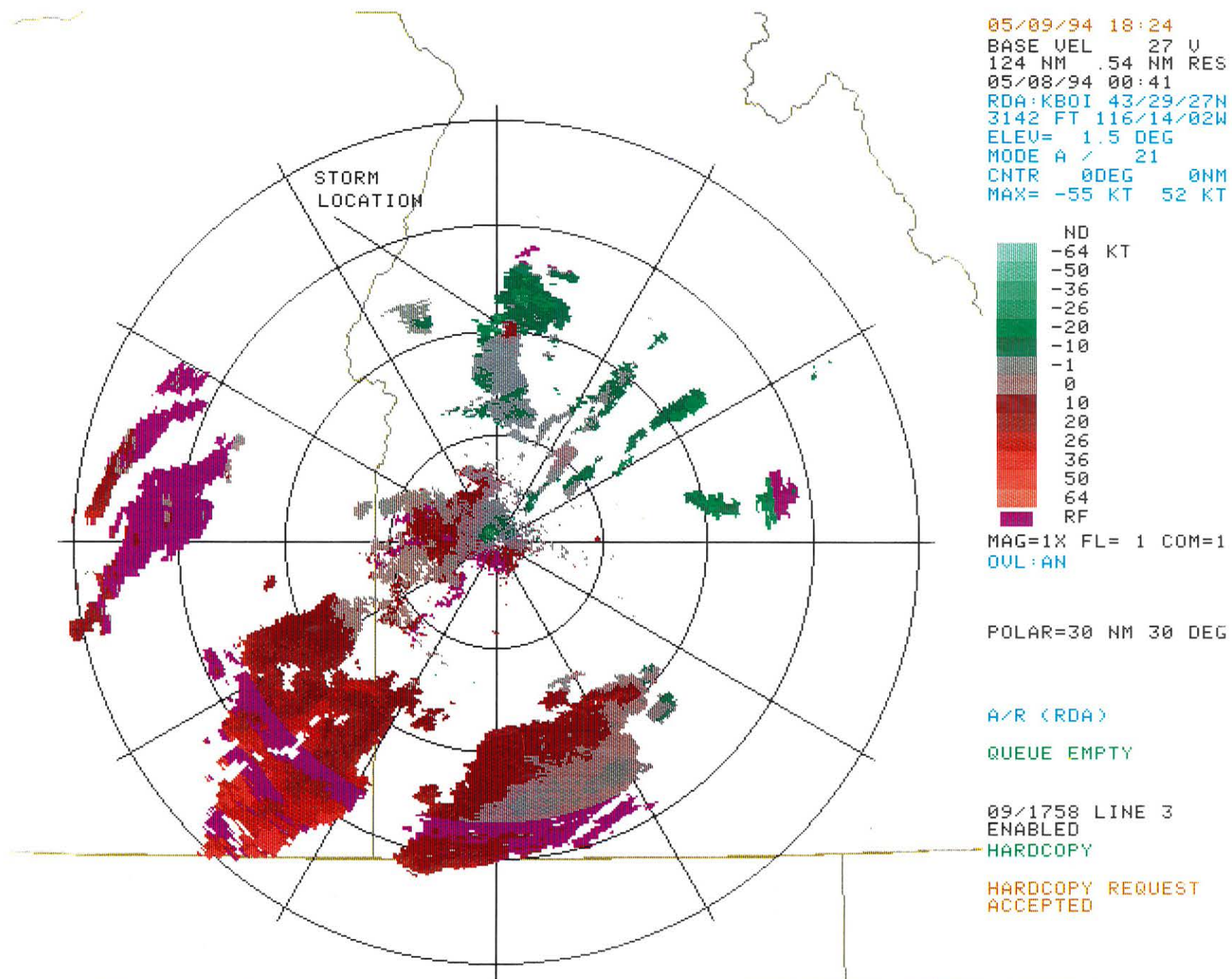


Figure 5. Base velocity data from the Boise WSR-88D at 0041 UTC, 8 May 1994. Elevation scan 1.5°. Range rings 30 km.

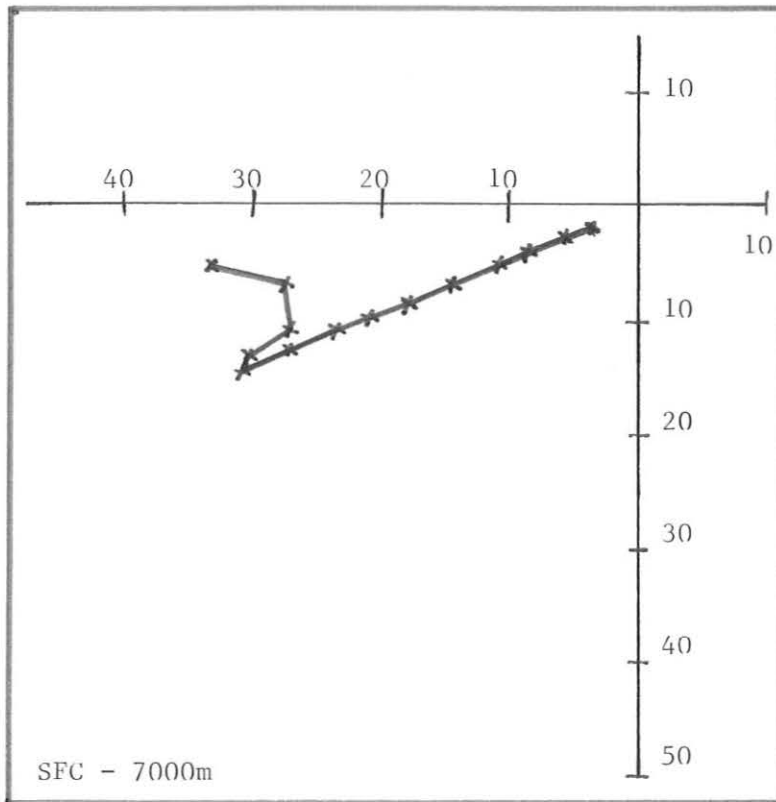


Figure 6. Hodograph based on winds from Boise 0000 UTC, 8 May 1994 rawinsonde. Wind plot from surface to 7000m at 500m intervals (intervals represented by the 'X's on the plot). Wind speeds in knots.

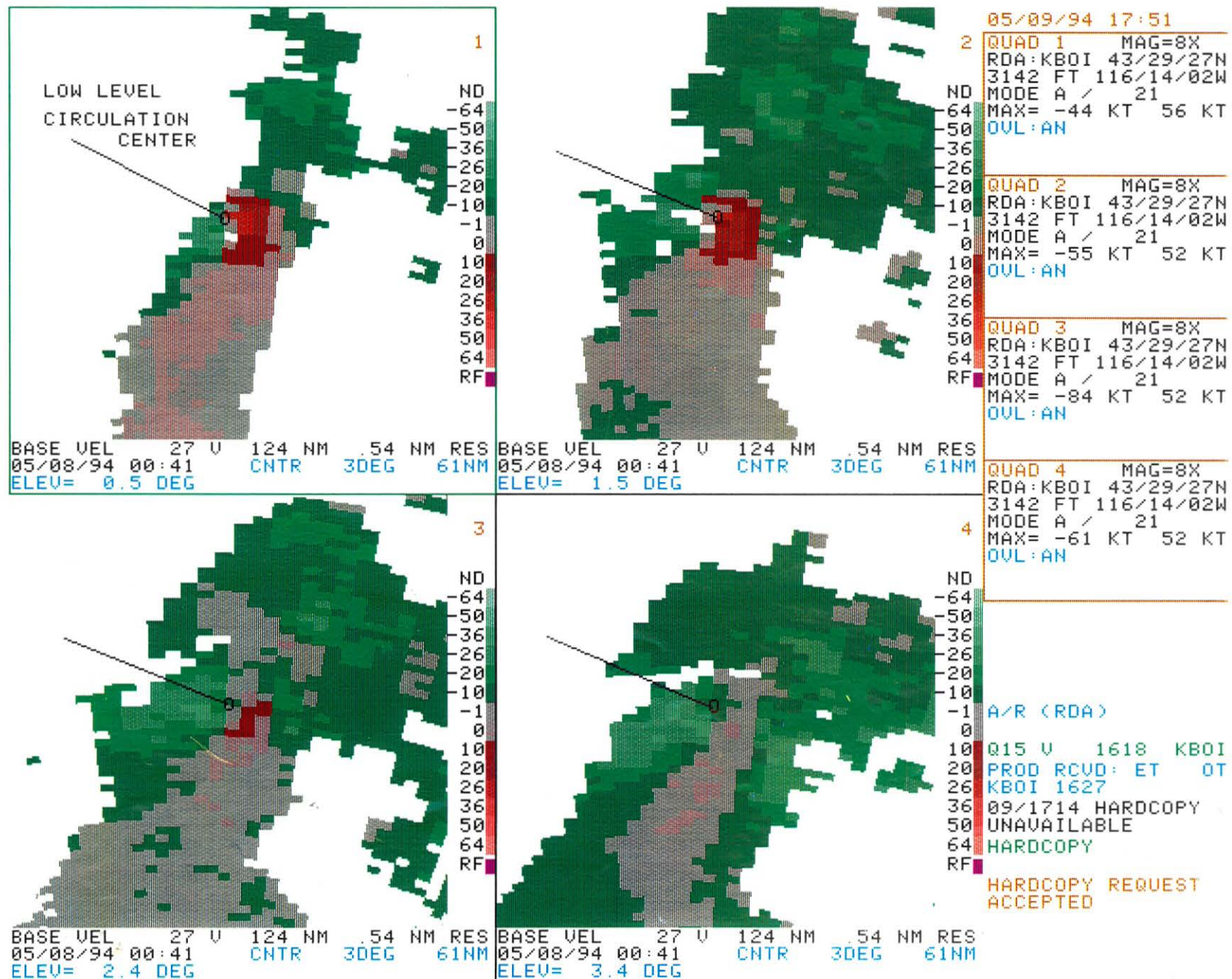


Figure 7. Base velocity data for 0041 UTC, 8 May 1994 at elevation scans (a) 0.5° (upper left), (b) 1.5° (upper right), (c) 2.4° (lower left), and (d) 3.4° (lower right). Images centered on supercell at an 8:1 magnification. Velocities in knots.

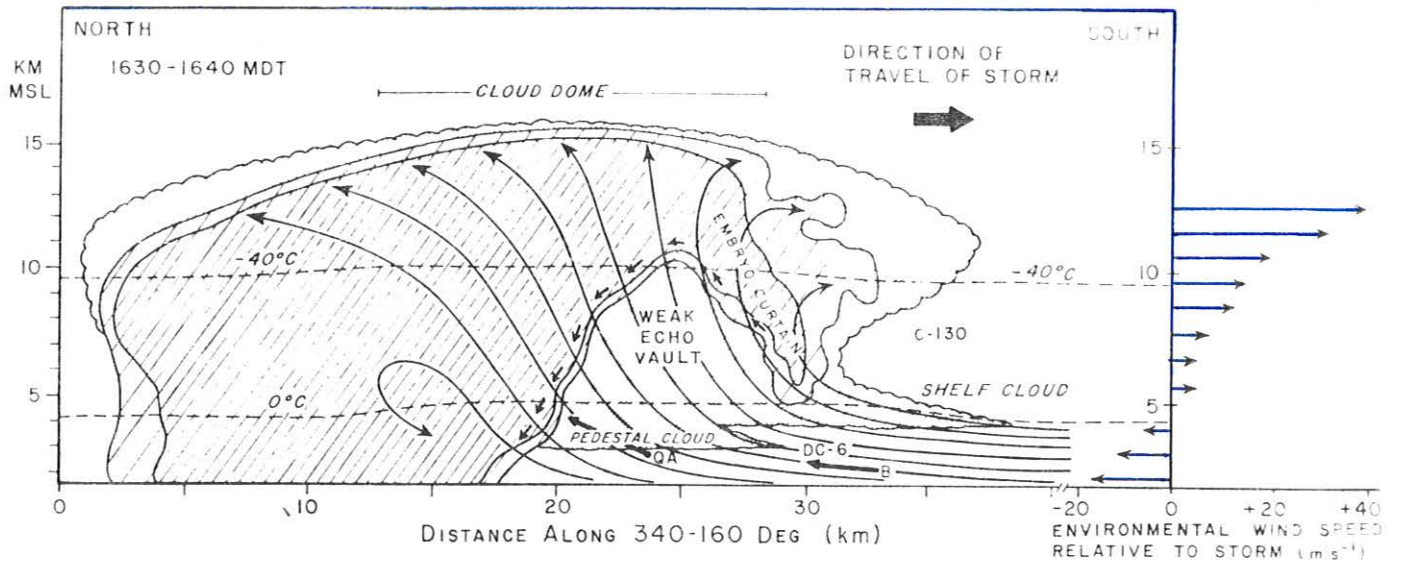


Figure 9. North-south cross-section of a classic supercell thunderstorm. The thin, solid lines are streamlines of airflow relative to the storm base. Note the strong updrafts within the region labeled "weak-echo vault" (Browning and Foote, 1976).

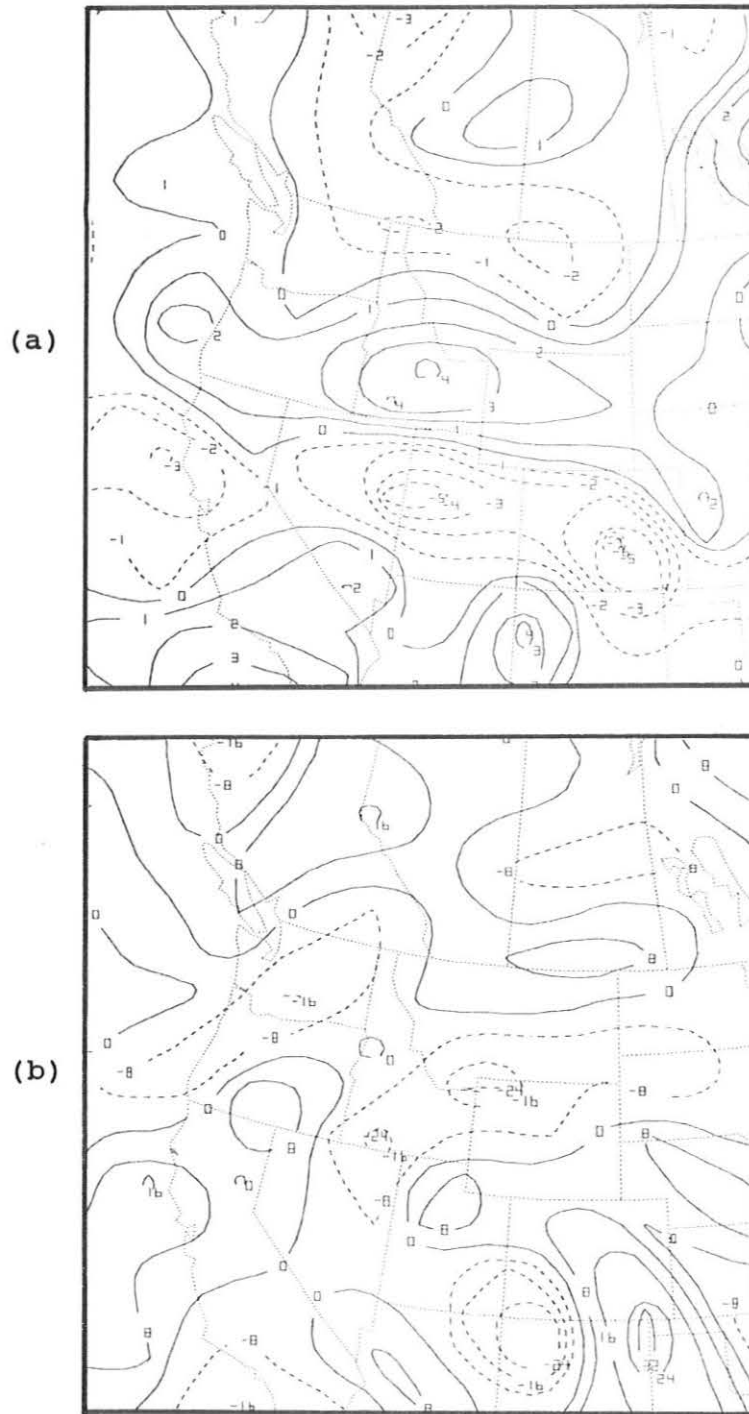


Figure 3. NGM 0000 UTC, 8 May, 1994 00 hour forecast of total wind divergence at (a) 300 mb, and (b) 700 mb. Positive (negative) values indicate divergence (convergence). Contour intervals $1 \times 10^{-5} \text{ s}^{-1}$ in (a) and $8 \times 10^{-6} \text{ s}^{-1}$ in (b).

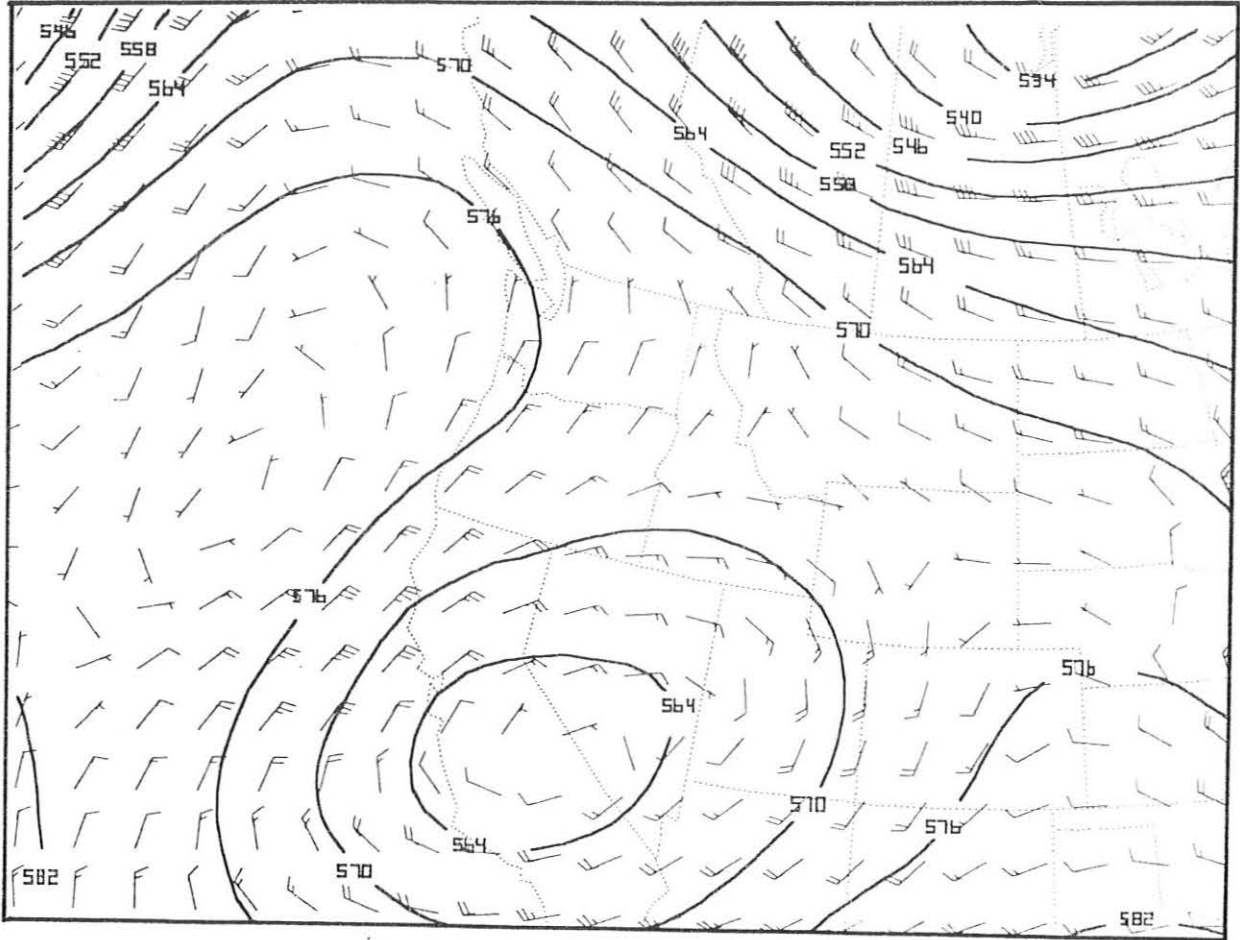


Figure 1. NGM 0000 UTC, 8 May, 1994 00 hour forecast of 500 mb heights (6 dam) and winds (m s^{-1}).

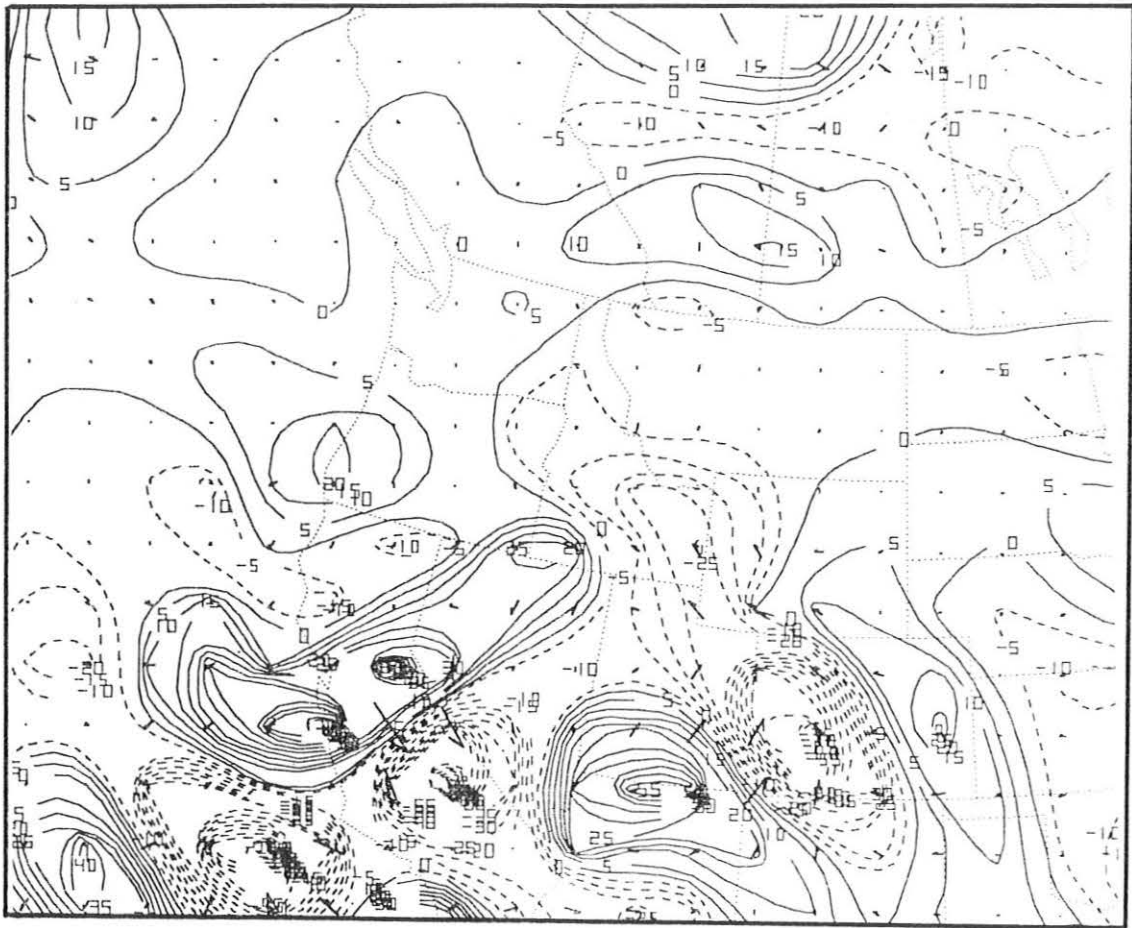


Figure 2. NGM 0000 UTC, 8 May, 1994 00 hour forecast of divergence of Q-vectors ($\nabla \cdot Q$) at 300 mb. Dashed (solid) contours represent convergence (divergence) of Q which corresponds to upward (downward) motion. Contour intervals $5 \times 10^{10} \text{ mb}^{-1} \text{ s}^{-3}$. Small arrows represent Q-vectors.